Contributions to Geophysics and Geodesy Vol. 42/1, 2012 (1–13)

Depth-dependent density change within the continental upper mantle

Robert TENZER[1], Mohammad BAGHERBANDI[2,3], Peter VAJDA[4]

[1] National School of Surveying, University of Otago
310 Castle street, Dunedin, 9054 New Zealand; e-mail: Robert.Tenzer@otago.ac.nz

[2] Division of Geodesy and Geoinformatics, Royal Institute of Technology (KTH)
10044 Stockholm, Sweden

[3] Department of Industrial Development, IT and Land Management
University of Gävle, 80176 Gävle, Sweden

[4] Geophysical Institute of the Slovak Academy of Sciences
Dúbravská cesta 9, 845 28 Bratislava, Slovak Republic; e-mail: geofvajd@savba.sk

Abstract: The empirical model of the depth-dependent density change within the upper continental mantle is derived in this study. The density of the upper(most) mantle underlying the continental crust is obtained from the estimated values of the crust–mantle (Moho) density contrast. Since the continental crustal thickness varies significantly, these upper mantle density values to a large extent reflect the density changes with depth. The estimation of the Moho density contrast is done through solving Moritz's generalization of the Vening-Meinesz inverse problem of isostasy. The solution combines gravity and seismic data in the least-squares estimation model. The estimated upper mantle density (beneath the continental crust) varies between 2770 and 3649 kg/m^3. The upper mantle density increases almost proportionally with depth at a rate of 13 ± 2 kg/m^3 per 1 km at the investigated depth interval from 6 to 58 km.

Key words: density interface, gravity, isostasy, mantle, Moho depths

1. Introduction

Seismic data were used for studying the Earth inner density structure. Theoretical foundations for these studies were given by *Williamson and Adams (1923)*. They formulated the relation between the Earth inner density and the velocities of the compressional (P-waves) and shear (S-waves) seismic waves. This functional relation is defined for the spherically symmetric, homogeneous Earth in hydrostatic equilibrium, while assuming the adiabatic

doi: 10.2478/v10126-012-0001-z

compression (meaning that thermal expansion does not contribute to density changes). According to this model the speed of seismic waves depends on the elastic properties of the Earth defined by the bulk modulus, shear modulus and density. The terms dependent on the adiabatic temperature gradients and on variations in chemical composition inside the Earth are usually disregarded. This relation was applied for a definition of the Earth seismic models. *Jeffreys and Bullen (1940)* and *Bullen (1940)* formulated the first density and seismic velocity profiles for entire Earth interior. *Bullen (1975)* compiled a more refined Earth density model. Currently the most commonly used (spherically symmetric) model is the Preliminary Reference Earth Model (PREM) compiled by *Dziewonski and Anderson (1981)*.

Results of seismic surveys have primarily been used also in global and regional geophysical studies investigating the lithosphere structure. *Soller et al. (1982)* derived the global seismic model of crustal thickness with a 2×2 arc-deg spatial resolution. The global crustal thickness model compiled with a spectral resolution complete to degree 30 of spherical harmonics was presented by *Čadek and Martinec (1991)*. *Nataf and Ricard (1996)* derived the global model of the crust and upper mantle density structure based on the analysis of seismic data and additional constrains such as heat flow and chemical composition. For global studies the most often used global crustal (and upper mantle) model is CRUST2.0 *(Bassin et al., 2000)*. CRUST2.0 was compiled and administered by the U.S. Geological Survey and the Institute for Geophysics and Planetary Physics at the University of California. CRUST2.0 is an upgrade of CRUST5.1 *(Mooney et al., 1998)*. Both models were compiled based on seismic data published until 1995 and a detailed compilation of ice and sediment thickness. A number of authors investigated the mantle structure based on the analysis of seismic data. We refer readers to global studies by *Dorman (1969), Silver and Chan (1991), Ita and Stixrude (1993), Li and Romanowicz (1996), Kaban and Schwintzer (2001), Poudjom Djomani et al. (2001), Zhao (2004), Zhou et al. (2006), Marone and Romanowicz (2007)*. The regional seismic studies of the mantle structure can be found, for instance, in *Burdick and Helmberger (1978), Iyer and Hitchcock (1989), Van der Lee and Nolet (1997), Snelson et al. (1998), Kaban and Mooney (2001), Marone et al. (2007), Nettles and Dziewonski (2008), Mooney and Kaban (2010)*, and others.

Over large areas of the world where seismic data are not yet available

or their spatial coverage is insufficient, the gravimetric or combined methods can be applied provided that the currently available global geopotential models have a high accuracy and resolution. *Sjöberg and Bagherbandi (2011)* developed and applied the combined least-squares model which combines information from seismic and gravity data in the isostatic inverse scheme for the simultaneous estimation of both Moho parameters. This method requires an optimal choice of the covariance matrix of known parameters for solving the system of normal equations. If both parameters are unknown, the problem has no unique solution. However, the least-squares solution can be found if the a priori estimates of the unknown parameters and their standard errors are known approximately.

If the density model of the upper mantle underlying the continental crust is available, it should be possible to estimate the depth-dependent (upper mantle) density changes due to the fact that the continental crustal thickness varies significantly. This principle is used here to establish an empirical relation between the upper mantle density and depth. The upper mantle density model beneath the continental crust is compiled using the Moho density contrast (relative to the homogeneous crustal model). The method developed by *Sjöberg and Bagherbandi (2011)* is applied to estimate the Moho density contrast.

2. Methodology

Sjöberg and Bagherbandi (2011) developed and applied the least-squares method for a simultaneous estimation of the Moho depths T and the Moho density contrast $\Delta\rho$ based on solving the inverse problem of isostasy and using the constraining information from seismic data. They formulated the linearised observation equation for the product $T\,\Delta\rho$ as follows:

$$T(\Omega)\,\Delta\rho(\Omega) = \sum_{n=0}^{N_{\max}} \sum_{m=-n}^{n} \left[\frac{2n+1}{4\pi G(n+1)} \Delta\tilde{g}^{i}_{n,m} - \frac{n+2}{2} (\Delta\rho T^2)_{n,m} \right] \times \\ \times\, Y_{n,m}(\Omega). \tag{1}$$

Equivalently, the observation equation for finding the Moho density contrast

$\Delta\rho$ based on given values of T reads (*ibid.*)

$$\Delta\rho(\Omega) = \frac{\Delta\tilde{g}^i(r,\Omega)}{2\pi\, G\, T(\Omega)} - \frac{1}{4\pi\, T(\Omega)} \sum_{n=0}^{N_{\max}} \sum_{m=-n}^{n} \left[\frac{1}{n+1} - \frac{T_0/R}{2/(n+2) - T_0/R}\right] \times$$

$$\times\, \Delta\tilde{g}^i_{n,m} Y_{n,m}(\Omega). \tag{2}$$

$G = 6.674 \times 10^{-11}\,\mathrm{m^3\,kg^{-1}\,s^{-2}}$ is the Newton gravitational constant; $R = 6371 \times 10^3\,\mathrm{m}$ is the Earth mean radius; $Y_{n,m}$ are the surface spherical harmonic functions; $\Delta\tilde{g}^i_{n,m}$ are the spherical harmonics of the (approximate) isostatic gravity anomalies $\Delta\tilde{g}^i$; $N_{\max}$ is the upper summation index of spherical harmonics; and T_0 is the adopted nominal mean value of the Moho depth. The 3-D position is defined in the system of spherical coordinates (r, Ω); where r is the spherical radius and $\Omega = (\phi, \lambda)$ denotes the spherical direction with the spherical latitude ϕ and longitude λ.

The least-squares analysis combines the estimated product of T and $\Delta\rho$ with the a priori values t and κ of these parameters in order to obtain the improved estimates of T and $\Delta\rho$. The system of observation equations, formulated for both parameters, is written in the following vector-matrix form:

$$\mathbf{A}\,\mathbf{x} = \mathbf{l} - \boldsymbol{\varepsilon}, \tag{3}$$

where $\boldsymbol{\varepsilon}$ is the vector of residuals. The system matrix $\mathbf{A}$, the parameter vector $\mathbf{x}$ and the observation vector $\mathbf{l}$ are given by

$$\mathbf{A} = \begin{pmatrix} \kappa & t \\ 0 & 1 \\ 1 & 0 \end{pmatrix}, \quad \mathbf{x} = \begin{pmatrix} \mathrm{d}T \\ \mathrm{d}\kappa \end{pmatrix}, \quad \mathbf{l} = \begin{pmatrix} l_1 - t\kappa \\ l_2 - t \\ l_3 - t \end{pmatrix}. \tag{4}$$

The elements l_1, l_2 and l_3, respectively, of the observation vector $\mathbf{l}$ are formed by the observables $T\,\Delta\rho$, $\Delta\rho$ and T. The parameter vector $\mathbf{x}$ consists of the unknown corrections $\mathrm{d}T$ and $\mathrm{d}\kappa$ to the a priori (initial) values of T and $\Delta\rho$. The solution is found based on solving the system of normal equations $\hat{\mathbf{x}} = \mathbf{N}^{-1}\mathbf{A}^{\mathrm{T}}\mathbf{Q}^{-1}\mathbf{l}$, where $\mathbf{N} = \mathbf{A}^{\mathrm{T}}\mathbf{Q}^{-1}\mathbf{A}$ is the normal matrix.

3. Data acquisition

The isostatic gravity anomalies in Eqs. (1) and (2) are computed in the spectral domain using the following expression (*Sjöberg, 2009*)

$$\Delta\tilde{g}^{i}_{n,m} = \frac{1}{4\pi}\begin{cases} 2\pi\, G\, (\bar{\rho}^{c}\, H)_{0,0} - \tilde{g}^{c}_{0} & \text{if} \quad n = 0 \\ 2\pi\, G\, (\bar{\rho}^{c}\, H)_{n,m} - \Delta g_{n,m} & \text{otherwise} \end{cases}, \tag{5}$$

where $\Delta g_{n,m}$ are the spherical harmonics of the gravity anomalies Δg; $2\pi\, G\, (\bar{\rho}^{c}\, H)_{n,m}$ is the spectral Bouguer gravity reduction term which is defined by means of the coefficients of global topographic/bathymetric (density) spherical functions $(\bar{\rho}^{c}\, H)_{n,m}$. The density distribution function $\bar{\rho}^{c}$ equals $\bar{\rho}^{c} = \rho^{c}$ on land, where ρ^{c} is the reference crustal density. The ocean density contrast is defined as $\bar{\rho}^{c} = \rho^{c} - \rho^{w}$; where ρ^{w} is the mean seawater density. The same definition is applied for any density contrast within the crust. The nominal compensation attraction (of zero-degree) $\tilde{g}^{c}_{0}$ stipulated at the sphere of radius R is computed as (cf. *Sjöberg, 2009*)

$$\tilde{g}^{c}_{0} = g^{c}_{0}\,(r, \Omega)\,|_{r=R} \approx -4\pi\, G\, \Delta\rho_{0}\, T_{0}, \tag{6}$$

where $\Delta\rho_{0}$ is the adopted nominal mean value of the Moho density contrast.

The global geopotential model EGM2008 (*Pavlis et al., 2008*), the global topographic/bathymetric model DTM2006.0 (*Pavlis et al., 2007*) and the global crustal model CRUST2.0 were used to compute the isostatic gravity anomalies. The global ice-thickness dataset was derived from Kort and Matrikelstyrelsen (KMS) ice data for Greenland (*Ekholm, 1996*) and assembled by the BEDMAP project for Antarctica (*Lythe et al., 2001*). All computations were realized globally on a 1×1 arc-deg grid at the Earth surface. The EGM2008 coefficients complete to the spherical harmonic degree 180 were used to generate the gravity anomalies. The refined Bouguer gravity anomalies were obtained after applying the (topographic and bathymetric) Bouguer gravity reduction to the EGM2008 gravity anomalies. The spherical Bouguer gravity reduction was computed using the coefficients of the global topographic/bathymetric model DTM2006.0 complete to the spherical harmonic degree 180. The average density of the upper continental crust 2670 kg/m^3 (cf. *Hinze, 2003*) was adopted as the topographic and reference crust densities. For the mean seawater density 1027 kg/m^3, the ocean density contrast equals 1643 kg/m^3. The ice stripping gravity correction was

computed with a spectral resolution complete to degree/order 180. The density of glacial ice 917 kg/m^3 (cf. *Cutnell and Kenneth, 1995*) was adopted for a definition of the ice density contrast of 1753 kg/m^3. The 2×2 arc-deg CRUST2.0 sediment data were used to compute the corresponding stripping gravity correction up to degree 90 of spherical harmonics. The computational models and global numerical results investigating the gravitational contributions of the crustal density structures can be found in *Tenzer et al., 2008; 2009a; 2009b; 2010a; 2010b; 2011a; 2011b).*

4. Results

The combined least-squares method was applied to estimate the crust–mantle density contrast. The solution was obtained by solving the system of normal equations. The observation vector $\mathbf{l}$ in Eq. (4) was composed of three observation types; namely $l_1 = T\,\Delta\rho$ (Eq. 1), $l_2 = \Delta\rho$ (Eq. 2), and $l_3 = T_S$ formed by the values of the CRUST2.0 Moho depths. The variance-covariance matrix $\mathbf{Q}$ used in the least-squares estimation model was computed as follows (cf. *Sjöberg and Bagherabndi, 2011*)

$$\mathbf{Q} = \begin{pmatrix} \sigma_1^2 & \sigma_1^2/t & 0 \\ \sigma_1^2/t & \sigma_2^2 & 0 \\ 0 & 0 & \sigma_3^2 \end{pmatrix}, \tag{7}$$

where σ_1 and σ_3 are the standard errors of the parameters $T\,\Delta\rho$ and T, respectively, and $\sigma_2^2 = \sigma_1^2/t^2 + \sigma_3^2\,(T\Delta\rho)^2\,/t^4$. The standard error σ_1 of $T\,\Delta\rho$ was computed using the following expression (*ibid.*)

$$\sigma_1^2 = \sigma_{T\Delta\rho}^2 \approx \left(\frac{\gamma_0}{4\pi G}\right)^2 \sum_{n,m} N_{n,m}^2\,\sigma_{n,m}^2 \quad , \tag{8}$$

where γ_0 is the GRS-80 normal gravity, $N_{n,m} = (2n+1)\,(n-1)/(n+1)$, and $\sigma_{n,m}^2$ are the error degree potential coefficients. Since the CRUST2.0 Moho depths data are not provided with the standard error model, we assumed the representative uncertainties (i.e., standard errors σ_3) in the Moho depth data of about 20% in the matrix $\mathbf{Q}$.

The estimated values of the Moho density contrast $\Delta\rho$ (taken relative to

the reference crustal density of 2670 kg/m^3) within the continental lithosphere computed on a 1×1 arc-deg grid vary between 100 and 979 kg/m^3 with a mean of 611 kg/m^3 and a standard deviation is 131 kg/m^3. The minima of the Moho density contrast within the continental lithosphere are found beneath the continental margins; here the values are typically 400–550 kg/m^3. The largest density contrast is found along the convergent tectonic plate boundaries. In particular, two locations of the maximum values correspond with the continent-to-continent collision zone in Himalayas (with extension under the Tibetan plateau) and with the ocean-to-continent subduction zone in Andes. According to our estimates, the maxima at these places exceed $\sim$ 800 kg/m^3. Large density contrast is also found beneath the east Antarctica, Greenland and the Rocky Mountains. Elsewhere beneath most of the continental crust the density contrast is usually 600–800 kg/m^3. The upper mantle density compiled globally on a 1×1 arc-deg grid from the estimated values of the Moho density contrast is shown in Fig. 1. Within the continental upper mantle, the density varies between 2770 and 3649 kg/m^3.

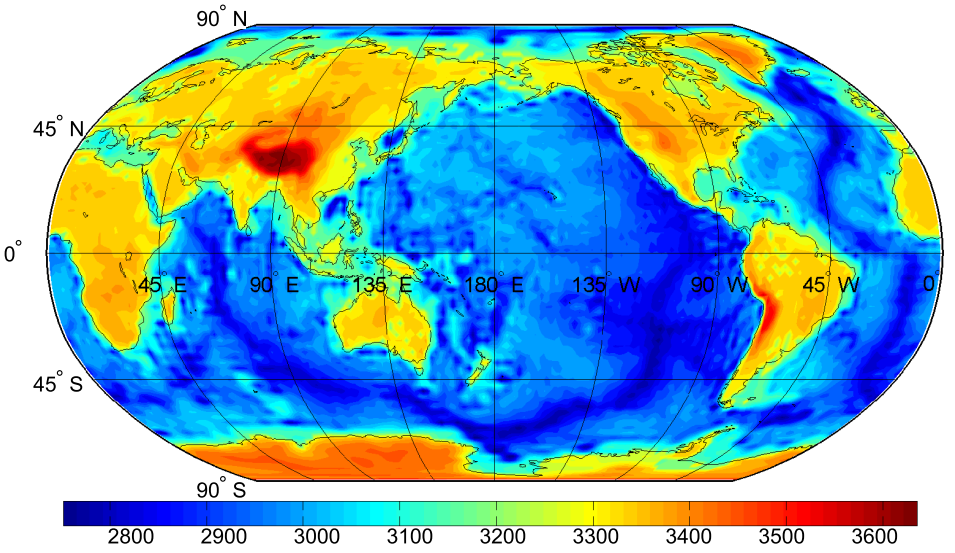

Fig. 1. Upper mantle lateral density computed globally on a 1×1 arc-deg grid. Units are in kg/m^3.

5. Continental upper mantle vertical density gradient

The upper mantle density beneath the continental crust is significantly correlated with the crustal thickness; the coefficient of determination (i.e., the square of a linear correlation coefficient) between these two quantities equals 0.68. The upper mantle density changes with depth within the continental lithosphere are plotted in Fig. 2. These values are taken at the interval of the Moho depths beneath the continental crust between 6 and 58 km.

As seen in Fig. 2, the upper mantle density almost proportionally increases with depth. The character of these density changes indicates that they are attributed mainly to pressure and geothermal gradient. The disper-

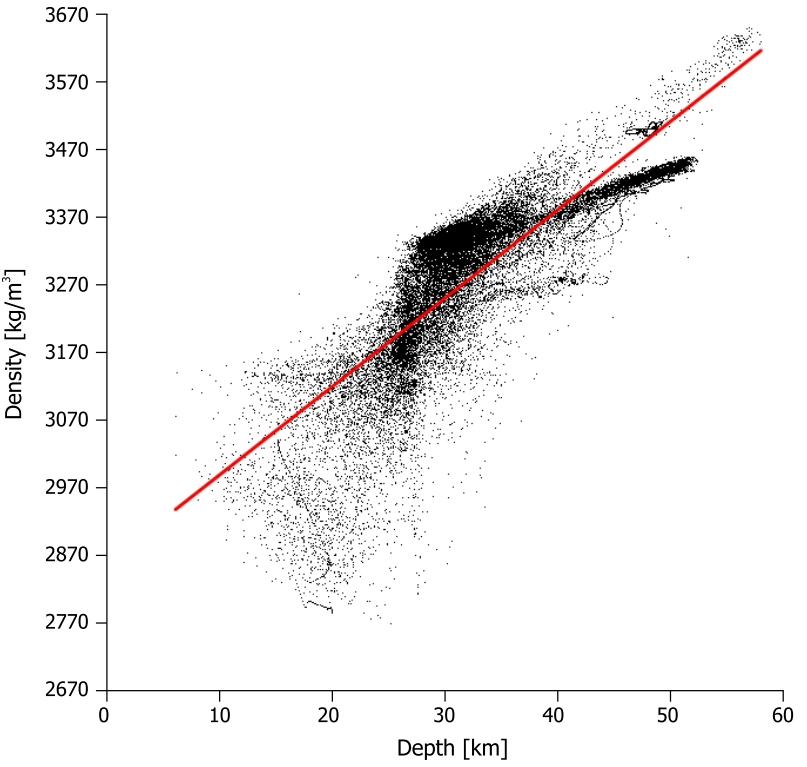

Fig. 2. Density changes with depth within the upper(most) mantle underlying the continental crust.

sions with respect to the systematic trend are caused by an inhomogeneous lateral density composition within the continental upper mantle as well as inaccuracies of the estimated depth and density values. The largest density dispersions (taken relative to the same depth) reach ~ 500 kg/m^3 at depths of 20–30 km. These dispersions substantially decrease with increasing depth to less than 100 kg/m^3 at depths below ~ 55 km. We further applied the least-squares analysis (for a linear regression fit) to estimate the empirical model of the depth-dependent density changes within the continental upper mantle. The estimated density gradient is 13 ± 2 kg/m^3 per 1 km.

This estimated density gradient does not agree with PREM density parameters. According to this model the density slightly decreases with depth (at a rate of 0.1 kg/m^3 per 1 km of depth) in the lithosphere and asthenosphere over the depth interval from 24.4 to 220 km. However, as discussed by *Stacey and Davis (1969)* the difficulty would arise even for zero density gradient. They estimated (based on using the relation between the pressure and temperature) that such density gradient would translate into unrealistically high temperatures at depth of 220 km. They argued that this discrepancy in PREM might be due to underestimating the effect of anisotropy in the asthenosphere, causing the inverted density gradient as a modeling artifact.

The accuracy of the estimated density gradient depends on several factors. The largest errors are attributed to the Moho depths and density contrast, both estimated simultaneously in the applied combined least-squares model. Moreover, additional errors are expected due to the fact that the lateral representation of the upper mantle density was determined merely based on the available crustal data without using any (constraining) information about the radial density changes within the upper mantle. Since the isostatic compensation does not take place only within the Earth crust (as it is assumed in classical isostatic hypothesis) but essentially also deeper in the lithospheric mantle (cf. *Kaban et al., 1999 and 2004; Vajda et al., 2007; Tenzer et al., 2009a and 2012*) there might be additional inaccuracies caused by theoretical limitations of the adopted isostatic model. The errors in estimated values of the Moho parameters (depths and density contrast) are attributed to inaccuracies of the input gravity and density structure data as well as to applied numerical approaches. Despite the standard errors of the Moho density contrast did not exceed 80 kg/m^3, the expected

real accuracy is much lower mainly due to unmodeled crustal structures. Moreover, the CRUST2.0 sediment data uncertainties decrease the accuracy especially beneath large continental sedimentary basins. The errors in the estimated Moho depths almost proportionally propagate into the errors of the estimated densities. According to the estimated density gradient the error of ± 1 km in the Moho depth corresponds to the density uncertainty of ± 13 kg/m^3.

The character of the upper mantle density variations under the oceanic lithosphere is significantly different (cf. Fig. 1). These density variations are attributed mainly to the mantle convection with a prevailing trend of increasing density with the age of oceanic lithosphere. The minima of the oceanic upper mantle density are detected along the mid-oceanic ridges, where the new oceanic lithosphere is formed. The density then increases as the older oceanic lithosphere is pushed away from the divergent oceanic tectonic plate boundaries. The density maxima are found along the subduction zones where the heaviest (and oldest) oceanic lithosphere is descending beneath either the continental or oceanic crust. The density changes with depth within the upper mantle underlying the oceanic crust are expected to be minor due to relatively small variations in the oceanic crustal thickness.

6. Summary and concluding remarks

We have established the empirical relation between the density and depth within the upper(most) mantle underlying the continental crust. The upper mantle density values at different depths used for the numerical analysis were determined from the estimated Moho parameters while adopting the constant reference crustal density.

The estimated density values of the upper continental mantle vary between 2770 and 3649 kg/m^3 with a mean of 3281 kg/m^3. The smallest values are located beneath the continental margins. The corresponding largest values are along the convergent tectonic plate boundaries in Himalayas (extending under the Tibetan plateau) and in Andes.

The density variations of the upper(most) mantle beneath the continental crust to a large extent reflect the density changes with depth. The coefficient of determination between the density and depth was found to be

0.68.

The continental upper mantle density almost proportionally increases with depth. According to our estimation, the density increases 13 ± 2 kg/m^3 per 1 km of depth.

Acknowledgments. First author was supported by the Project No. 76/10:1 of the Swedish National Space Board (SNSB). Peter Vajda was supported by the Slovak Research and Development Agency under the contract No. APVV-0194-10 and by Vega grant agency under projects No. 2/0067/12 and 1/0095/12.

References

Bassin C., Laske G., Masters T. G., 2000: The current limits of resolution for surface wave tomography in North America. EOS Trans AGU, **81**, F897.

Bullen K. E., 1940: The problem of the Earth's density variation. Bull. Seis. Sic. Amer., **30**, 235–250.

Bullen K. E., 1975: The Earth's Density. Chapman and Hall, London.

Burdick L. J., Helmberger D. V., 1978: The upper mantle P-velocity structure of the western United States. J. Geophys. Res., **83**, B4, 1699–1712.

Cutnell J. D., Kenneth W. J., 1995: Physics, 3$^{\text{rd}}$ Edition, Wiley, New York.

Čadek O., Martinec Z., 1991: Spherical harmonic expansion of the earth's crustal thickness up to degree and order 30. Studia Geoph. et Geod., **35**, 151–165.

Dorman J., 1969: Seismic surface-wave data on the upper mantle. In: The Earth's Crust and Upper Mantle. AGU Geophys. Monogr Ser., **13**, (Eds.) Hart P. J., 257–265, AGU, Washington, D.C.

Dziewonski A. M., Anderson D. L., 1981: Preliminary Earth Reference Model. Phys. Earth Planet. Inter., **25**, 297–356.

Ekholm S., 1996: A full coverage, high-resolution, topographic model of Greenland, computed from a variety of digital elevation data. J. Geophys. Res., **B10**, 21, 961–972.

Ita J., Stixrude L., 1993: Density and elasticity of model upper mantle compositions and their implications for whole mantle structure. In: Evolution of the Earth and Planets, Geophys. Monogr. Ser., **74**, (Eds.) Takahashi E., Jeanloz R., Rubie D., 111–130, AGU, Washington, D. C.

Iyer H. M., Hitchcock T., 1989: Upper-mantle velocity structure in the continental U.S. and Canada. In: Geophysical Framework of the Continental United States, Geol. Soc. Am. Mem., **172**, (Eds.) Pakiser L. C., Mooney W. D., 681–710, Geol. Soc. Am., Boulder, Colo.

Jeffreys H., Bullen K. E., 1940: Seismological Tables. Brit. Ass. Gray-Milne Trust.

Hinze W. J., 2003: Bouguer reduction density, why 2.67? Geophysics, **68**, 5, 1559–1560.

Kaban M. K., Schwintzer P., Tikhotsky S. A., 1999: Global isostatic gravity model of the Earth. Geophys. J. Int., **136**, 519–536.

Kaban M. K., Mooney W. D., 2001: Density structure of the lithosphere in the southwestern United States and its tectonic significance. *J. Geophys. Res.*, **106**, 721–740.

Kaban M. K., Schwintzer P., 2001: Oceanic upper mantle structure from experimental scaling of V_s and density at different depths. Geophys. J. Int., **147**, 199–214.

Kaban M. K., Schwintzer P., Reigber Ch., 2004: A new isostatic model of the lithosphere and gravity field. J. Geod., **78**, 368–385.

Li X., Romanowicz B., 1996: Global mantle shear velocity model developed using nonlinear asymptotic coupling theory. J. Geophys. Res., **101**, B10, 22,245–22,272.

Lythe M. B., Vaughan D. G., BEDMAP consortium, 2001: BEDMAP; a new ice thickness and subglacial topographic model of Antarctica. J. Geophys. Res., B, Solid Earth Planets, **106**, 6, 11,335–11,351.

Marone F., Romanowicz B., 2007: The depth distribution of azimuthal anisotropy in the continental upper mantle. Nature, **447**, 198–201.

Marone F., Gung Y., Romanowicz B., 2007: Three-dimensional radial anisotropic structure of the North American upper mantle from inversion of surface waveform data. Geophys. J. Int., **171**, 206–222.

Mooney W. D., Laske G., Masters T. G., 1998: CRUST 5.1: a global crustal model at 5x5 deg. J. Geophys. Res., **103**, 727–747.

Mooney W. D., Kaban M. K., 2010: The North American upper mantle: Density, composition, and evolution. J. Geophys. Res., **115**, B12424.

Nataf H. C., Ricard Y., 1996: 3SMAC: An a priori tomographic model of the upper mantle based on geophysical modeling. Phys. Earth Planet. Int., **95**, 101–122.

Nettles M., Dziewonski A. M., 2008: Radially anisotropic shear velocity structure of the upper mantle globally and beneath North America. J. Geophys. Res., **113**, B02303.

Pavlis N. K., Factor J. K., Holmes S. A., 2007: Terrain-Related Gravimetric Quantities Computed for the Next EGM. In: Gravity Field of the Earth. A. Kiliçoglu and R. Forsberg (Eds.), Proceedings of the 1st International Symposium of the International Gravity Field Service (IGFS), Harita Dergisi, Special Issue No. 18, General Command of Mapping, Ankara, Turkey.

Pavlis N. K., Holmes S. A., Kenyon S. C., Factor J. K., 2008: An Earth Gravitational Model to Degree 2160: EGM 2008, presented at Session G3: "GRACE Science Applications", EGU Vienna.

Poudjom Djomani Y. H., O'Reilly S. Y., Griffin W. L., Morgan P., 2001: The density structure of subcontinental lithosphere through time. Earth Planet. Sci. Lett., **184**, 605–621.

Silver P. G., Chan W. W., 1991: Shear-wave splitting and subcontinental mantle deformation. J. Geophys. Res., **96**, B10, 16,429–16,454.

Sjöberg L. E., 2009: Solving Vening Meinesz-Moritz Inverse Problem in Isostasy. Geophys. J. Int., **179**, 3, 1527–1536.

Sjöberg L. E., Bagherbandi M., 2011: A Method of Estimating the Moho Density Contrast with A Tentative Application by EGM08 and CRUST2.0. Acta Geophysica, **59**, 3, 502–525.

Snelson C. M., Henstock T. J., Keller G. R., Miller K. C., Levander A., 1998: Crustal and uppermost mantle structure along the Deep Probe seismic profile. Rocky Mountain Geology, **33**, 181–198.

Soller D. R., Richard D. R., Richard D. B., 1982: A new global crustal thickness map. Tectonics, **1,** 145–149.

Stacey F. D., Davis P. M., 1969: Earth, density distribution. In: The Earth's crust and upper Mantle: structure, dynamic processes, and their relation to deep-seated geological phenomena. (Ed.) Hart P. J., American Geophysical Union, Washington, D. C., Geophysical Monograph 13, Upper Mantle Project Scientific Report 21, 133–137.

Tenzer R., Hamayun, Vajda P., 2008: Global map of the gravity anomaly corrected for complete effects of the topography, and of density contrasts of global ocean, ice, and sediments. Contrib. Geophys. Geod., **38**, 4, 357–370.

Tenzer R., Hamayun, Vajda P., 2009a: Global maps of the CRUST2.0 crustal components stripped gravity disturbances. J. Geophys. Res., **114**, B, 05408.

Tenzer R., Hamayun, Vajda P., 2009b: A global correlation of the step-wise consolidated crust-stripped gravity field quantities with the topography, bathymetry, and the CRUST 2.0 Moho boundary. Contrib. Geophys. Geod., **39**, 2, 133–147.

Tenzer R., Vajda P., Hamayun, 2010a: A mathematical model of the bathymetry-generated external gravitational field. Contrib. Geophys. Geod., **40**, 1, 31–44.

Tenzer R., Abdalla A., Vajda P., Hamayun, 2010b: The spherical harmonic representation of the gravitational field quantities generated by the ice density contrast. Contrib. Geophys. Geod., **40**, 3, 207–223.

Tenzer R., Novák P., Gladkikh V., 2011a: On the accuracy of the bathymetry-generated gravitational field quantities for a depth-dependent seawater density distribution. Studia Geophys. Geodaet., **55**, 4, 609–626.

Tenzer R., Hamayun, Novák P., Gladkikh V., Vajda P., 2011b: Global crust-mantle density contrast estimated from EGM2008, DTM2008, CRUST2.0, and ICE-5G. Pure Appl. Geophysics, doi:10.1007/s00024-011-0410-3.

Tenzer R., Gladkikh V., Vajda P., Novák P., 2012: Spatial and spectral analysis of refined gravity data for modelling the crust-mantle interface and mantle-lithosphere structure. Surveys in Geophysics, doi:10.1007/s10712-012-9173-3.

Vajda P., Vaníček P., Novák P., Tenzer R., Ellmann A., 2007: Secondary indirect effects in gravity anomaly data inversion or interpretation. J. Geophys. Res., **112**, B, 06411.

Van der Lee S., Nolet G., 1997: Upper mantle S velocity structure of North America. J. Geophys. Res., **102**, B10, 22,815–22,838.

Williamson E. D., Adams L. H., 1923: Density distribution in the Earth. J. Wash. Acad. Sci., **13**, 413–428.

Zhao D. P., 2004: Global tomographic images of mantle plumes and subducted slabs: Insight into deep Earth dynamics. Phys. Earth Planetary Inter., **146**, 3–24.

Zhou Y., Nolet G., Dahlen F. A., Laske G., 2006: Global upper-mantle structure from finite-frequency surface-wave tomography. J. Geophys. Res., **111**, B04304.